

Accepted Manuscript

Transition metal complexes with thiosemicarbazide-based ligands. Part 63.
Syntheses, structures and physicochemical characterization of the first chromium(III) complexes with pyridoxal semi- and thiosemicarbazones

Ljiljana S. Vojinović-Ješić, Ljiljana S. Jovanović, Vukadin M. Leovac, Mirjana M. Radanović, Marko V. Rodić, Berta Barta Holló, Katalin Mészáros Szécsényi, Sonja A. Ivković

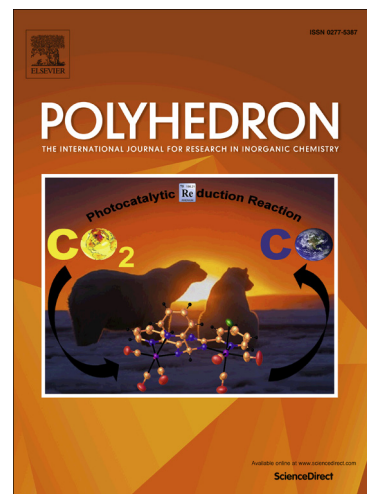
PII: S0277-5387(15)00519-7
DOI: <http://dx.doi.org/10.1016/j.poly.2015.09.017>
Reference: POLY 11531

To appear in: *Polyhedron*

Received Date: 1 July 2015
Accepted Date: 5 September 2015

Please cite this article as: L.S. Vojinović-Ješić, L.S. Jovanović, V.M. Leovac, M.M. Radanović, M.V. Rodić, B.B. Holló, K.M. Szécsényi, S.A. Ivković, Transition metal complexes with thiosemicarbazide-based ligands. Part 63. Syntheses, structures and physicochemical characterization of the first chromium(III) complexes with pyridoxal semi- and thiosemicarbazones, *Polyhedron* (2015), doi: <http://dx.doi.org/10.1016/j.poly.2015.09.017>

This is a PDF file of an unedited manuscript that has been accepted for publication. As a service to our customers we are providing this early version of the manuscript. The manuscript will undergo copyediting, typesetting, and review of the resulting proof before it is published in its final form. Please note that during the production process errors may be discovered which could affect the content, and all legal disclaimers that apply to the journal pertain.



Transition metal complexes with thiosemicarbazide-based ligands. Part 63. Syntheses, structures and physicochemical characterization of the first chromium(III) complexes with pyridoxal semi- and thiosemicarbazones

Ljiljana S. Vojinović-Ješić^a, Ljiljana S. Jovanović^a, Vukadin M. Leovac^{a*}, Mirjana M. Radanović^a, Marko V. Rodić^a, Berta Barta Holló^a, Katalin Mészáros Szécsényi^a, Sonja A. Ivković^b

^a Faculty of Sciences, University of Novi Sad, Trg Dositeja Obradovića 3, 21000 Novi Sad, Serbia

^b Faculty of Environmental Protection, University EDUCONS, V. Putnika bb, 21208 Sremska Kamenica, Serbia

Abstract

With pyridoxal semi-/thiosemicarbazones (PLSC/PLTSC) ligands for the first time chromium complexes were obtained. In the reaction of ethanolic solution of $\text{Cr}(\text{NO}_3)_3$ and $\text{K}_3[\text{Cr}(\text{NCS})_6]$ and the ligands in mole ratio 1:1 or 1:2, the following complexes were formed: $[\text{Cr}(\text{PLSC})(\text{PLSC}-\text{H})(\text{NO}_3)_2 \cdot \text{H}_2\text{O}]$ (**1**), $\text{K}[\text{Cr}(\text{PLSC}-\text{H})(\text{NCS})_3] \cdot \text{EtOH}$ (**2**), $[\text{Cr}(\text{PLTSC})(\text{PLTSC}-\text{H})(\text{NO}_3)_2 \cdot 2\text{H}_2\text{O}]$ (**3**), $[\text{Cr}(\text{PLTSC})_2](\text{NO}_3)_3$ (**4**) and $[\text{Cr}(\text{PLTSC})(\text{NCS})_3] \cdot 2\text{H}_2\text{O}$ (**5**). All the complexes have *mer*-octahedral structure which in the cases of the complexes **2**, **4** and **5** was proved by single-crystal X-ray diffraction analysis. The Schiff bases coordinate in the usual tridentate ONX manner (X=O/S; PLSC/PLTSC). The pyridoxalic fragment is zwitter ion regardless of the form of the coordinated ligands: neutral (keto/thion) and monoanionic (enolic/thiolic). In addition to the above complexes, X-ray crystallography was used to characterize neutral and protonated forms of PLSC, i.e. $\text{PLSC} \cdot 2\text{H}_2\text{O}$ and $\text{PLSC} \cdot \text{HNCS}$, the latter one being obtained as a by-product of the reaction of formation of the complex **2** using $\text{K}_3[\text{Cr}(\text{NCS})_6]$ and PLSC in the mole ratio 1:2. The X-ray analyses of these ligand forms have shown that in the case of $\text{PLSC} \cdot \text{HNCS}$ the ligators $\text{O}_{\text{phenolic}}$, $\text{N}_{\text{azomethine}}$, O_{keto} due to strong hydrogen $\text{O}_2\text{-H} \cdots \text{N}_3$ bond are placed in *cis*-position to each other (pro-binding conformation) which is not the case with $\text{PLSC} \cdot 2\text{H}_2\text{O}$. The compounds are characterized thoroughly by also IR/UV-Vis spectral analyses, electrochemical and thermal methods.

Keywords

pyridoxal semi-/thiosemicarbazone, chromium(III) complexes, crystal structure, spectra, thermal decomposition, electrochemistry

* Corresponding author. E-mail address: vukadin.leovac@dh.uns.ac.rs (V.M. Leovac)

1. Introduction

Chromium has an important role in metabolism of two primary macronutrients—carbohydrates and lipides [1], but is also one of the most controversial transition metals in the view of its biological activity [2]. The latter is due to the toxicity of Cr(VI), which exists in the form of oxyanion, and as such can easily enter the cells and lead to formation of reactive oxygen species [3]. In contrast, Cr(III) appeared to be more stable and less cytotoxic to cultured human cells [4], while the insufficiency of Cr(III) in organism causes diabetes and some cardiovascular diseases [1].

On the other hand, semi- and thiosemicarbazones and their metal complexes are interesting compounds not only in theoretical view [5–8], but due to the possibility of their practical application as biologically active molecules [9, 10], analytical reagents [11, 12], etc. Among them, semi- and thiosemicarbazones of pyridoxal (PLSC and PLTSC, respectively), which is one of the forms of vitamin B6, are particularly interesting. These ligands and their complexes stand out in many ways: biological activity [13–15], and interesting and diverse physicochemical and structural characteristics [13, 16–19]. Since there are no complexes of Cr(III) with these Schiff bases and considering the biological importance of both the Cr(III) and ligands, it is of considerable interest to synthesize and characterize their complexes.

2. Experimental

2.1. Materials and physical measurements

All commercially obtained reagent-grade chemicals were used without further purification. The ligand PLTSC was prepared according to the previously described procedure [19], while the single crystals of the ligand PLSC·2H₂O were obtained in a slightly modified procedure compared with the one described in [20], since the previously known one have not yielded in formation of single crystals.

Elemental analyses (C, H, N and S) of air-dried compounds were carried out by standard micro-methods in the Center for Instrumental Analyses, ICTN in Belgrade. Molar conductivity measurements of freshly prepared 1 mM solutions were performed on a Jenway 4010 conductivity meter. IR spectra were recorded on a Nicolet Nexus 670 FTIR (Thermo Scientific) spectrophotometer, in the range of 400–4000 cm⁻¹ by KBr pellet technique. Electronic spectra of DMF solutions of the ligand and complexes were recorded on a T80+ UV/Vis Spectrometer (PG Instruments, Ltd.), in the spectral range of 270–1000 nm. Cyclic voltammetric experiments were carried out on a VOLTALAB PST050 with a GC-disk (diameter 3 mm) working electrode, Pt wire counter electrode and a reference saturated calomel electrode (SCE). All potentials are reported against this electrode. The measurements were carried out in analytical grade DMF solvent which was double distilled after prior drying on molecular sieves. Supporting electrolytes were 0.1 M tetrabutylammonium perchlorate (TBAP) or LiClO₄. Experiments were carried out in an inert atmosphere provided by purging nitrogen. Thermal data were recorded in the

temperature range to 600 °C using TA Instruments' Q600 SDT Thermal Analyser coupled online with Hiden HAL RC 301 quadrupole mass spectrometer. Selected ions between $m/z = 1-100$ were monitored in multiple ion detection mode (MID). Measuring parameters: sample masses ~ 5 mg; heating rate 10 °C min⁻¹; argon atmosphere (flow rate 50 cm³ min⁻¹); alumina sample and empty alumina reference pan. Simultaneous thermogravimetric (TG) and differential scanning calorimetric (DSC) measurements were carried out under similar conditions but at a heating rate of 20 °C min⁻¹ in flowing nitrogen. Selected samples were tested in air atmosphere, too.

2.2. Syntheses

2.2.1. PLSC·2H₂O

Semicarbazide hydrogenchloride (1.07 g, 10 mmol) was dissolved in warm H₂O (10 mL), to which a warm solution of pyridoxal hydrogenchloride (2.00 g, 10 mmol) in H₂O (10 mL) was added. To this solution Na₂CO₃·10H₂O (3.00 g, 15 mmol) dissolved in H₂O (10 mL) was added in portions, and the mixture was mildly heated for a couple of minutes. The obtained solution was left at room temperature for about 20 h, after which the single crystals were filtered and washed with H₂O. Yield: 2.30 g (88%). *Anal.* Calc. for C₉H₁₆N₄O₅: C, 41.54; H, 6.20; N, 21.53. Found: C, 41.43; H, 6.16; N, 21.50%. Selected IR bands [$\tilde{\nu}$ /cm⁻¹]: 3466, 3381, $\nu(\text{OH})$, $\nu(\text{NH}_2)$; 3202, $\nu(\text{NH})$; 2850, $\nu(\text{NH}^+)$; 1697, 1678, $\nu(\text{C}=\text{O})$; 1583, $\nu(\text{CN})$; 1280, $\nu(\text{CO}_{\text{phenolic}})$. UV-Vis (DMF) [$\lambda_{\text{max}}/\text{nm}$ (log $\epsilon/\text{M}^{-1} \text{cm}^{-1}$)]: 289 (4.12), 298sh (4.08), 327bp (3.75). (sh-shoulder, bp-broad peak)

2.2.2. [Cr(PLSC)(PLSC-H)](NO₃)₂·H₂O (1)

Cr(NO₃)₃·9H₂O (100 mg, 0.25 mmol) was poured with hot EtOH (10 mL) and the warm suspension of PLSC·2H₂O (130 mg, 0.5 mmol) in EtOH (10 mL) was added. This mixture was slightly heated until the ligand was completely dissolved. After 24 hours red-brown microcrystals were filtered and washed with EtOH and dried *in vacuo*. Yield: 60 mg (38%). *Anal.* Calc. for C₁₈H₂₅CrN₁₀O₁₃: C, 33.71; H, 3.93; N, 21.84. Found: C, 33.29; H, 9.95; N, 21.57%. Conductivity [$\Lambda_{\text{M}}/\Omega^{-1} \text{cm}^2 \text{mol}^{-1}$]: 130 (in DMF). Selected IR bands [$\tilde{\nu}/\text{cm}^{-1}$]: 3436, 3302, $\nu(\text{OH})$, $\nu(\text{NH}_2)$; 3215, $\nu(\text{NH})$; 2850, $\nu(\text{NH}^+)$; 1669, $\nu(\text{C}=\text{O})$; 1637, $\nu(\text{CN})$; 1384, $\nu(\text{NO}_3)$; 1300, $\nu(\text{CO}_{\text{phenolic}})$; 1250, $\nu(\text{CO}_{\text{enolic}})$. UV-Vis (DMF) [$\lambda_{\text{max}}/\text{nm}$ (log $\epsilon/\text{M}^{-1} \text{cm}^{-1}$)]: 307 (4.23), 324 (4.20), 359 (4.17), 428 (4.24), 475sh (3.89), 629 (2.20), 699 (2.0), 774 (1.74).

2.2.3. K[Cr(PLSC-H)(NCS)₃]·EtOH (2); PLSC·HNCS

The mixture of K₃[Cr(NCS)₆]·4H₂O (250 mg, 0.5 mmol) and PLSC·2H₂O (130 mg, 0.5 mmol) was poured with EtOH (10 mL) and refluxed for 5 h on 90 °C. The obtained dark-red solution was left at the room temperature and after 5 days dark-red laminar single crystals of the complex were precipitated. Yield: 160 mg (59%). Under the same reaction conditions but at the molar ratio 1:2, as an admixture yellow monocrystals of the ligand PLSC·HNCS were formed. *Anal.* Calc. for KC₁₄H₁₇CrN₇O₄S₃: C, 31.45; H, 3.21; N, 18.34; S, 17.99. Found: C, 31.25; H, 3.19; N, 18.35; S, 18.03%. For chemical check of potassium see SI. Conductivity [$\Lambda_{\text{M}}/\Omega^{-1} \text{cm}^2$

mol^{-1}): 17 (in DMF); 23 (in MeOH). Selected IR bands [$\tilde{\nu}/\text{cm}^{-1}$]: 3462, 3333, $\nu(\text{OH})$, $\nu(\text{NH}_2)$; 2924, $\nu(\text{NH}^+)$; 2072, $\nu(\text{NCS})$; 1666, $\nu(\text{CN})$; 1331, $\nu(\text{CO}_{\text{phenolic}})$; 1246, $\nu(\text{CO}_{\text{enolic}})$. UV–Vis (DMF) [$\lambda_{\text{max}}/\text{nm}$ ($\log \epsilon/\text{M}^{-1} \text{cm}^{-1}$)]: 308 (4.33), 366sh (3.96), 421bp (3.80), 445 (3.78), 483 (3.32), 556 (2.30), 708 (1.49), 784(1.11).

2.2.4. $[\text{Cr}(\text{PLTSC})(\text{PLTSC}-\text{H})](\text{NO}_3)_2 \cdot 2\text{H}_2\text{O}$ (3)

The mixture of $\text{Cr}(\text{NO}_3)_3 \cdot 9\text{H}_2\text{O}$ (100 mg, 0.25 mmol) and PLTSC (120 mg, 0.5 mmol) was heated in EtOH (20 mL) under reflux for 4h on 80 °C. After 24h staying at the room temperature from red-brown solution brown micro-crystals were filtered and washed with EtOH. Yield: 130 mg (37%). *Anal. Calc.* for $\text{C}_{18}\text{H}_{27}\text{CrN}_{10}\text{O}_{12}\text{S}_2$: C, 31.26; H, 3.93; N, 20.25; S, 9.27. Found: C, 31.39; H, 3.52; N, 20.65; S, 9.12%. Conductivity [$A_{\text{M}}/\Omega^{-1} \text{cm}^2 \text{mol}^{-1}$]: 110 (in DMF). Selected IR bands [$\tilde{\nu}/\text{cm}^{-1}$]: 3318, 3273, $\nu(\text{OH})$, $\nu(\text{NH}_2)$; 3164, $\nu(\text{NH})$; 2950–2800, $\nu(\text{NH}^+)$; 1607, $\nu(\text{CN})$; 1384, $\nu(\text{NO}_3)$; 841, $\nu(\text{CS})$. UV–Vis (DMF) [$\lambda_{\text{max}}/\text{nm}$ ($\log \epsilon/\text{M}^{-1} \text{cm}^{-1}$)]: 316 (4.27), 360sh (4.05), 465 (3.81), 507 (3.30), 713sh (1.49), 792sh (1.20)

2.2.5. $[\text{Cr}(\text{PLTSC})_2](\text{NO}_3)_3$ (4)

A few single crystals of this complex were obtained from the mother liquor of the previously described complex (3).

2.2.6. $[\text{Cr}(\text{PLTSC})(\text{NCS})_3] \cdot 2\text{H}_2\text{O}$ (5)

The mixture of 250 mg (0.5 mmol) $\text{K}_3[\text{Cr}(\text{NCS})_6] \cdot 4\text{H}_2\text{O}$ and PLTSC (120 mg, 0.5 mmol) was poured with EtOH (10 mL) and heated under reflux for 4h at 85 °C. After 7 days dark-red rod-like single crystals were filtered and washed with EtOH. Yield: 110 mg (42%). *Anal. Calc.* for $\text{C}_{12}\text{H}_{16}\text{CrN}_7\text{O}_4\text{S}_4$: C, 28.68; H, 3.21; N, 19.51; S, 25.52. Found: C, 28.56; H, 3.20; N, 19.43; S, 25.42%. Conductivity [$A_{\text{M}}/\Omega^{-1} \text{cm}^2 \text{mol}^{-1}$]: 26 (in DMF). Selected IR bands [$\tilde{\nu}/\text{cm}^{-1}$]: 3479, 3430, 3248, $\nu(\text{OH})$, $\nu(\text{NH}_2)$; 3162, $\nu(\text{NH})$; 2916, 2849, $\nu(\text{NH}^+)$; 2110, 2096, $\nu(\text{NCS})$; 1615, $\nu(\text{CN})$; 1307, $\nu(\text{CO})$; 828, $\nu(\text{CS})$. UV–Vis [$\lambda_{\text{max}}/\text{nm}$ ($\log \epsilon/\text{M}^{-1} \text{cm}^{-1}$)]: 316 (4.27), 360sh (4.05), 465 (3.81), 507 (3.30), 713sh (1.49), 792sh (1.20)

2.3. X-ray crystal structure determination

Diffraction measurements at room temperature were performed on an Oxford Diffraction Gemini S diffractometer equipped with Sapphire3 CCD detector. Diffraction data were collected using graphite monochromatized Cu $K\alpha$ radiation ($\lambda = 1.5418 \text{ \AA}$) for all structures, with the exception of complex **5**, for which Mo $K\alpha$ radiation ($\lambda = 0.71073 \text{ \AA}$) was used. Data collection, integration, scaling and absorption corrections were processed using the *CRYALISPRO* [21]. Structures were solved using *SHELXT* [22]. The full-matrix least-squares refinement based on F^2 was performed with *SHELXL-2014* [23] integrated in the *SHELXLE* graphical user interface [24]. All non-H atoms were refined anisotropically. C-bonded H-atoms are introduced in idealized positions and refined as riding on parent atoms, while O and N-bonded H-atoms were taken from difference Fourier maps and refined with distance restraints. U_{iso} of all H-atoms were

evaluated from U_{eq} of their parent atoms. In the structure of PLSC·HNCS hydroxyl group was modeled as disordered over two sites. In the structure of **2**, ethanol molecule was modeled as disordered over two sites with hydrogen atoms generated in idealized positions. Distance and ADP similarity restraints were applied to maintain chemically reasonable geometry. Structures were validated using *PLATON* [25], and Cambridge Structural Database (CSD) (v. 5.36, updates Nov. 2014) [26] using *MERCURY CSD 3.5* [27]. Crystal data and refinement parameters of ligands and the complexes are given in Table 1.

Crystallographic data for complexes **2**, **4**, **5**, and ligands PLSC·2H₂O, PLSC·HNCS, have been deposited with the Cambridge Crystallographic Data Centre as Supplementary publication Nos. CCDC 1408327–1408331, respectively. A copy of these data can be obtained, free of charge, via <https://summary.ccdc.cam.ac.uk/structure-summary-form>, or by emailing data_request@ccdc.cam.ac.uk.

3. Results and discussion

3.1. Syntheses and characterization

Scheme 1 shows the synthetic routes to the Cr(III) complexes. All complexes are obtained in the reactions of warm EtOH solutions of Cr(NO₃)₃·9H₂O or K₃[Cr(NCS)₆]·4H₂O with PLSC·2H₂O and PLTSC, respectively. In case of reactions of Cr(NO₃)₃·9H₂O with ligands the molar ratio was 1:2, and cationic bis(ligand) complexes **1**, **3** and **4** with neutral and monoanionic form of the ligands are obtained. The reactions of K₃[Cr(NCS)₆]·4H₂O with the ligands regardless of the stoichiometry (1:1 or 1:2) yielded in only mono(ligand) complexes **2** and **5**, whilst in the reaction of PLSC with K₃[Cr(NCS)₆] in molar ratio 2:1, in addition to the mono(ligand) complex **2**, single crystals of PLSC·HNCS are isolated.

The complexes and ligands are stable in air. All complexes are well soluble in DMF and MeOH and poorly soluble in EtOH. Unlike the electrolyte-type complexes (**1**, **2**, **3** and **4**) which are soluble in H₂O, solubility of **5** is poor.

Molar conductivities of complexes **1** and **3** in DMF are in accordance with their proposed coordination formulas (i.e. 2:1 type of electrolyte), while conductivity of **2** is lower and that of **5** somewhat higher than expected [28].

3.2. IR and electronic spectra

In these complexes, the ligands are coordinated in a tridentate *ONO/ONS* mode, via oxygen atom of phenolic OH-group, nitrogen atoms of azomethine and oxygen/sulphur atom of amide/thioamide group –C(–NH₂)=X (X = O, S). In the case of complexes **2**, **4** and **5** this was confirmed by the single-crystal X-ray analysis (*vide infra*).

IR spectra of the complexes are in accordance with the afore mentioned ligand coordination modes. Thus, in the spectra of all complexes, due to the phenolic oxygen coordination, $\nu(\text{CO}_{\text{phen}})$ band which in the spectra of the ligands is at ca 1285 cm⁻¹, is positively shifted for 20–40 cm⁻¹ [19, 29–31]. Upon coordination, the band originating from $\nu(\text{CN})$

vibrations of azomethine group, which is in the spectra of the ligands present at 1583 (PLSC) and 1540 cm^{-1} (PLTSC), is shifted toward high energy region (1618–1666 cm^{-1}) [19, 32, 33].

The carbonyl oxygen coordination can be confirmed by the band of high intensity ascribed to $\nu(\text{C}=\text{O})$ vibrations that is in the spectrum of complex **1** moved to lower energies (1669 cm^{-1}) compared to the spectrum of PLSC (1697 and 1676 cm^{-1}). The absence of this band in mono-PLSC complex (**2**), as well as the absence of hydrazinic $\nu(\text{NH})$ band in the range 2200–2120 cm^{-1} confirm the monoanionic (enolic) form of the ligand. In the spectra of this, as well of **1**, which contain one molecule of PLSC in monoanionic (enolic) form, the band $\nu(\text{CO}_{\text{enolic}})$ is located at 1242 and 1250 cm^{-1} , respectively [34–36]. In the spectra of complexes with PLTSC, the $\nu(\text{CS})$ band, found in lower energy region (ca 835 cm^{-1}) compared with the spectrum of the ligand (923 cm^{-1}) alone, suggests the coordination *via* the sulphur atom [19, 32].

Beside the above mentioned bands, in spectra of complexes some additional bands can be assigned. Thus, in the spectra of all complexes, as well as of both ligands, one or more bands of different intensities in the range between 2950 and 2800 cm^{-1} correspond to $\nu(\text{NH}^+)$ vibrations of the protonated pyridine nitrogen of PL moiety [32, 37]. Finally, in the spectra of the complexes **1** and **3** a very strong band attributed to $\nu(\text{NO}_3)$ vibrations is present at 1384 cm^{-1} , while the spectra of complex **2** contain the band at 2072 cm^{-1} , which can be assigned to $\nu(\text{CN})$ vibrations of isothiocyanato ligand [38]. This band in the spectrum of complex **5** is present as doublet (2096 and 2110 cm^{-1}).

When the electronic spectra are concerned, although the ligands absorb in one (PLTSC) or two (PLSC) mainly well defined absorption bands [39], their Cr(III) complexes show more complicated spectral picture. In DMF all the complexes have spectra with unresolved absorptions in high-energy region, where the ligand $\pi \rightarrow \pi^*$ absorption bands are red-shifted upon complexation. In addition, several charge-transfer bands appear down to 540 nm with high intensity. Finally, d–d transitions are better resolved at PLSC complexes than at PLTSC ones. Their number and intensities witness about distorted geometries of the octahedral Cr(III) complexes.

3.3. Crystal structures of PLSC·2H₂O and PLSC·HNCS

Table 2 summarizes pertinent structural data for PLSC·2H₂O and PLSC·HNCS, whereas molecular structures are shown in Figure 1. The main difference in the structures of the ligands is that in case of PLSC·HNCS the conformation suitable for coordination is achieved, so that both ligating O2 and O1 atoms are *cis* with respect to hydrazinic ligating atom N3, whereas the neutral ligand PLSC·2H₂O has conformations in which both O2 and O1 atoms are *trans* with respect to hydrazinic N3. It appears that the nature of PL moiety strongly affects the conformation of the molecules in a similar way as it was found in thio-analogues of PLSC (PLTSC) [31]. Namely, due to the protonation of phenolic OH-group and the existence of a strong intramolecular O2–H2A···N3 bond (Table S1, Supplementary material), the ligand PLSC·HNCS is stabilized in pro-binding conformation. In contrast to this, no such hydrogen

bond is possible in the neutral ligand, since H-atom from phenolic group has migrated to nitrogen atom of PL fragment forming the zwitter-ion.

The different nature of the PL moiety in two molecules implies some differences in the bond lengths, such as the elongation ($\approx 0.04 \text{ \AA}$) of C4–O2 in the cation compared with the molecule of the neutral ligand. In both structures C1–O1 bond has a value close to the one characteristic for double C=O bond, while C1–N1 and C1–N2 bonds have partial double bond character. The value of C5–N4–C7 angle is ca 124° which is in line with the protonation of nitrogen atom of PL moiety [37].

3.4. Crystal structures of complexes **2**, **4**, and **5**

Selected structural data for complexes **2**, **4**, and **5** are summarized in Table 2, whereas the molecular structures are shown in Figure 2. All structurally characterized complexes have *mer*-octahedral structure, which is in case of the complexes **2** and **5** realized by coordination of an ONX tridentate ligand ($X = \text{O}$ in **2** and $X = \text{S}$ in **5**), and three NCS^- ions, while in **4** the coordination sphere is comprised of two ONS ligand molecules. It should be noted that complexes where octahedral coordination of Cr(III) is achieved by three NCS^- ions and one tridentate ligand as found in **2** and **5** are very rare. The search of CSD (v. 5.36 update Nov. 2014) shows that there are only two such complexes, namely $(\text{HL}^1)[\text{Cr}(\text{L}^1\text{-H})(\text{NCS})_3]\cdot\text{MeOH}$ and $[\text{Cr}(\text{L}^2)(\text{NCS})_3]\cdot\text{DMF}$, where $\text{L}^1 = 1\text{-}(2\text{-pyridyldiazanyl})\text{-}2\text{-naphtholate}$ and $\text{L}^2 = 4'\text{-}(2\text{-pyridyl})\text{-}2,2':6',2''\text{-terpyridine}$ [40, 41]. In complex **2** the potassium ion is situated in highly deformed pentagonal bipyramidal environment made by three oxygen atoms at distance 2.840(5)–2.878(4) \AA (two oxygens of ethanol molecules, one oxygen of hydroxymethyl group), and three sulfur atoms belonging to coordinated thiocyanate ions at distances 3.2900(15) to 3.4606(17) \AA . The search of the CSD reveals that hitherto there are no examples where ethanol and thiocyanate ion are simultaneously bonded to potassium ions, however there are several compounds in which either ethanol or thiocyanate are coordinated (see Supplementary information for list of corresponding CSD Refcodes). The lengths of K–S and K–O bonds in **2** are in expected range if compared to the distances found in the mentioned examples.

In all the complexes the ligands PLSC and PLTSC are coordinated in the usual tridentate manner, i.e. through oxygen atom of phenolic group, nitrogen of azomethine and carbonyl oxygen (PLSC), i.e. sulphur (PLTSC) by forming six-membered pyridoxylidene and five-membered semi/thiosemicarbazide metalocycles. The pyridoxalic fragment in all three complexes is in the form of dipolar zwitter-ion, which is not surprising because these ligands in their free (non-coordinated) forms are zwitter-ions. In line with zwitter-ionic structure is the value of the angle between the pyridine nitrogen atom and the neighbouring carbon atoms in these complexes (ca 124°) [31, 37]. In complex **2** PLSC is coordinated as monoanion, in which the deprotonation of hydrazinic nitrogen (N2) takes place.

Of two mutual metal–chelate ligand bonds (Cr1–O2/N3) significantly shorter one is Cr1–O2 (av. 1.92 \AA) compared to Cr1–N3 (av. 2.03 \AA). This is in accordance with the literature data regarding not only these but also the complexes of other metals with these ligands [13]. Very

similar bond length to Cr1–N3 have also virtually identical Cr1–NCS bonds (av. 2.00 Å) which is in accordance with those found in [40, 41]. When Cr1–O1 bond (1.9802(19) Å) is concerned, it is very close to that of the octahedral Cr(III) complex with semicarbazones of salicyl/pyridine-2-carbaldehyde, i.e. 2.011(3) Å [42] and 1.997(3) Å [43], respectively. The lengths of Cr1–S1 bonds in both PLTSC complexes have the values similar to those found in also octahedral complexes of Cr(III) with tridentate thiosemicarbazone ligands [2, 44].

A comparative analysis of the lengths of intraligand bonds in free neutral and coordinated ligands in addition of great likeness shows in the case of PLSC the differences regarding primarily the ureido fragment $-N^2H-C^1(=O^1)N^1H_2$. Namely, due to deprotonation of this fragment, i.e. the hydrazinic N2 atom, the C1–N2 bond significantly shortens (1.329(4) Å) in comparison to the same in the free ligand (1.371(4) Å). Consequently, the C1–O1 bond which in the free ligand has a character of a double bond (1.247(4) Å), in the complex is elongated (1.301(4) Å) becoming similar to C–O enolato bonds in other complexes [43, 45–48].

The lengths of C4–O2 phenolato bonds in free and coordinated ligands are almost identical: (1.29 Å (free ligands) and 1.30 Å (coordinated ligands)). In the case of PLSC, the azomethine C2–N3 bond after coordination prolongs by 0.02 Å unlike PLTSC where this bond remains virtually unchanged. The latter regards also the C=S bonds [2].

Even though the ligands alone are almost planar [32], due to the formation of the metallocycles, they deviate significantly from planarity in complexes **4** and **5**, whereas in **2** the degree of planarity is on the contrary very high. This structural feature of **4** and **5** can be described by the values of appropriate dihedral/torsion angles (Table 2). The mean plane of pyridine ring is inclined to the mean plane through donor atoms of the chelate ligand and Cr1 which can be judged from the values of the appropriate dihedral angle δ (Table 2). In both complexes all chelate rings are puckered. Six-membered metallocycles have conformation close to twist- or screw-boat with the largest torsion angle $\tau(C3-C4-O2-Cr1)$, while the five-membered metallocycles are twisted on Cr1–N3 or have a conformation of an envelope on Cr1, with the largest torsion angle $\tau(C1-N2-N3-Cr1)$ (puckering parameters are given in Table S2, Supplementary material). The observed deviation from planarity upon coordination has much resemblance with those found in transition metal complexes with similar pyridoxal semi- and non-substituted and substituted thiosemicarbazones (see for example [49, 50]), noting that deviation in complex **4** tends to extreme values.

3.5. Electrochemistry

Ligands

Both ligands reduce in one $1-e^-$ process at the potentials -1.51 V (PLSC) and -1.37 V (PLTSC). The processes are quasi-reversible and diffusion-controlled. After reduction, new pairs of $1-e^-$ peaks arise at the more negative potentials: -1.88 V (PLSC) and -1.97 V (PLTSC) which are due to slow chemical reactions. On the basis of our previous results for a similar ligand (pyridoxal aminoguanidine), it can be supposed that the first process is located at the pyridoxal moiety [51], while the second one corresponds with the first reduction of the

semicarbazone and thiosemicarbazone fragments, respectively [52–54]. The first reduction peaks have $I_p/cv^{1/2} \sim \text{const}$ and $\Delta E_p/\Delta \log v \sim -40 \text{ mV decade}^{-1}$ which is consistent with the presence of a following chemical reaction. Oxidation occurs in a multielectron process at the potentials more positive than +1.0 V followed by irreversible chemical reactions of ligand decomposition. Addition of five-fold excess of lithium acetate to the ligands' solution to form deprotonated ligand did not affect much their reduction processes, while a dramatic change appeared at the positive potentials: new complex oxidation peaks at potentials between +0.15 V and +0.50 V appeared in a similar way with those recorded for some other semicarbazone-based ligands [52]. The obtained species have strong adsorption affinities.

Complexes

The two types of complexes, mono- and bis-ligand, differ in their voltammetric behavior, both in appearance and electrochemical characteristics.

The voltammograms of the mono(ligand) thiocyanate complex **2** are shown in Figure 3a. As can be seen, generally two reduction (I and II) and one oxidation process (Ox) can be observed. In the widest potential amplitude the processes characteristic for the coordinated ligand oxidation or reduction are also recorded with parameters similar to those of the free ligand.

The two reduction processes have characteristics of consecutive $1-e^-$ transfers followed by chemical reactions. A deeper insight into the process at the peak I reveals that it is composed of two close peaks which are results of electronation of the species involved in the equilibrium with NCS^- . A more detailed picture can be obtained with variation of the potential amplitude and sweep rate: if the potential is reversed after the peak I, at higher scan rates the presence of instable species can be recorded both around the peak I' and at more positive potentials (Figure 3b). Of the two oxidation peaks in the region of the peak I' ($v = 2 \text{ V s}^{-1}$), the more negative one is the counterpart of the reduced starting complex, i.e. of $[\text{Cr}(\text{PLSC-H})(\text{NCS})_3]^{2-}$ that is prone to relax an excess of negative charge by releasing 1–2 NCS^- . In this way the complex with a possible composition $[\text{Cr}(\text{PLSC-H})(\text{NCS})_n(\text{DMF})_{3-n}]^{1-n}$ is formed which oxidizes at somewhat more positive potentials. With lowering the scan rate below 0.5 V s^{-1} this species dominates and under suitable conditions of amplitude and sweep rate a new slightly more positive reduction process (for about 50 mV) can be observed in the second sweep (Figure 3). In parallel with this, the free NCS^- reacting in the peak Ox, according to the current parameters which are dependent both on the sweep rate and the potential amplitude, seems to be involved in two opposed chemical reactions. First, fast release after reduction of Cr^{III} complex leading to an increase of the peak Ox. Then, after reoxidation of Cr^{II} to Cr^{III} species in peak I', a much slower reaction of its recoordination to form the starting compound is occurring which results in decreasing the peak Ox.

The peak I current function $I_p/cv^{1/2} \sim \text{const}$; peak potential variation $\Delta E_p/\Delta \log v \sim -30 \text{ mV decade}^{-1}$ (measured as first sweep). Current functions of the peaks II and I, i.e. $I_p(\text{II})/I_p(\text{I})$ range from ~ 1 at low sweep rates to ~ 0.8 at $v > 0.5 \text{ V s}^{-1}$. The peak Ox has

complex behavior: $I_p(\text{Ox})/I_p(\text{I})$ decreases both at low and at high scan rates, reaching its maximal value of 1.5 at $v = 0.20 \text{ V s}^{-1}$ for the smaller amplitude (down to -1.0 V). In the wider amplitude (to -1.6 V) this parameter increases to a value of 3 which points to a more pronounced NCS^- releasing effect at negative potentials.

In order to establish the effect of the presence of NCS^- on the composition and behavior of the reacting species, we added the stoichiometric amount of Ag^+ to precipitate the anion. As the result, a new pair of quasi-reversible peaks at the potential $E^{0'} = -0.55 \text{ V}$ (at 100 mV s^{-1} $\Delta E_p^{a/c} = 80 \text{ mV}$) was formed with a possible composition of the reactant: $[\text{Cr}^{\text{III}}(\text{PLSC-H})(\text{DMF})_3]^{2+}$. In parallel with this, the peak II remained practically unchanged, while the peak Ox disappeared. On the basis of this, we suppose that in the peak II reacts mainly the NCS^- -free complex.

Generally similar, but less stable complex behavior was observed for mono(ligand) PLTSC complex. A comparison of the voltammograms for the two NCS^- complexes is shown in Figure 4. The main difference is recorded in the potential range of the peak II where up to three small peaks arise depending on the sweep rate. A peculiarity of this complex in DMF is that free NCS^- is present in the solution regardless the reduction process. Its current in the amplitude 0.0 V to $+0.9 \text{ V}$ is practically the same as after reduction at the peak I. This might be the result of the present NCS^- acting to prevent its further dissociation from the reduced complex. When the peak II process is concerned, it is less defined, since in this particular potential range even three small peaks appear. They may be ascribed to the reactions of both the NCS^- -containing and NCS^- -free Cr^{II} species, while the most negative one might be due to the free ligand (see above).

The bis(ligand) complexes show ill-defined voltammograms with several small peaks, at the potentials ranging from -0.5 V till -1.5 V (Figure 5). On the basis of a similarity with the NCS^- -complexes, we suppose that the first two peaks (around -0.6 V) correspond to reactions of the mono(ligand) species, while the other two to the bis(ligand) ones. To check this assumption, we added the equivalent amount of $\text{K}_3[\text{Cr}(\text{NCS})_6]$ to form the mono(ligand) complex. After this addition to the PLSC complex solution, the resulted voltammogram had all previously described peaks for the mono(ligand) NCS^- complex at the characteristic potentials. However, a deeper insight into the nature of these processes for the bis(ligand) complexes is not easy to acquire and, because of their instabilities in DMF, probably not of scientific interest.

3.6. Thermal decomposition

As thermoanalytical methods belong to standard methods for characterization of potentially bioactive compounds giving information on their thermal stability, the type and amount of the solvent, the possible polymorphic transformations [55] or purity [56–58], the compounds were characterized by coupled TG/MS measurements, too.

According to the elemental analysis data all compounds contain crystal water except of complex **2** which crystallizes with ethanol and **4** that crystallizes without any solvent. The solvent evaporation starts practically at room temperature in all the compounds. Only **PLSC·2H₂O** has a relatively high water evaporation temperature ($114 \text{ }^\circ\text{C}$ onset).

The solvent content of **PLSC**·2H₂O (exp. 14.1 %; calcd. 13.84 %) and its complexes **1** (exp. 2.7 %; calcd. 2.81 %), **2** (exp. 8.4 % to the minimum in DTG curve; calcd. 8.62 %) agrees well with the calculated value. The anhydrous ligand and complex **1** are stable over a 70 °C temperature range (to 208 °C and 233 °C onsets, respectively). Compound **2** starts to decompose before the evaporation of EtOH is completed. The decomposition of the desolvated compounds is continuous in the whole temperature range taking place practically in one step for **PLSC** ligand and **1** while **2** decomposes in a stepwise manner.

PLTSC obtained here does not contain crystal water, however, it is hygroscopic binding about 2 % water (exp. 1.9 %). The water content of its complexes **3** and **5** is less than the stoichiometric one (exp. 2.5 % – calcd. 5.21 %; exp 5.8 % – calcd. 7.17 %, respectively) which is not surprising according to the relatively low onset temperature of dehydration. The stability of the dehydrated **PLTSC** and **3** is also relatively high (onsets: 218 °C, 260°C, respectively) while the anhydrous **5** is stable to 191 °C. The following decomposition proceeds with better separated but still overlapping steps compared to the corresponding **PLSC** compounds. The comparison of the decomposition of the compounds is illustrated by the corresponding DTG curves presented in Figure 6a and b.

TG/MS data refer to the complete water evaporation up to ~160 °C. The peak for nitrate ion appears at $m/z = 30$ amu (NO⁺) in nitrate compounds (**1** and **3**) while in thiocyanates peak for HNCS⁺ at $m/z = 59$ amu (**2** and **4**) has been found, in accordance with the proposed/determined molecular structure. From the ethanolic solvate, **2**, peaks for EtOH (CH₃O⁺, C₂H₅O⁺, CH₂O⁺ and C₂H₅OH with decreasing intensity, in the accordance with literature data [59]) refer to its complete evaporation above 250 °C only, where the fragmentation of the organic ligand is already in progress (see Figure 7).

As the ligand molecules are rich in oxygen atoms, peaks for water appear not only at lower temperatures in hydrates (< 180 °C) but also above 200 °C because oxygen atoms in the molecules oxidize the fragments at elevated temperatures to H₂O and CO₂ ($m/z = 44$). In addition, in **PLTSC** compounds there are peaks at $m/z = 48$ (SO⁺) and 64 amu (SO₂) characteristic for the ligand decomposition.

As hydrates with **PLTSC** lose the crystal water at room temperature, they should be dried at ~120 °C to constant mass prior to elemental analysis in order to check the stoichiometry/homogeneity of the batches. Compound **2** is not stable; therefore its potential practical applicability is probably seriously restricted. DSC curves do not refer to any structural changes or melting of the compounds. However, melting accompanied with the decomposition was observed in all compounds.

Conclusions

With chromium(III) and tridentate Schiff bases pyridoxal semi/thiosemicarbazones five complexes were obtained as the first complexes of this metal with the cited ligands. Using Cr(NO₃)₃ solely the cationic bis(ligand) complexes containing both neutral and monoanionic ligand form were isolated, while by means of K₃[Cr(NCS)₆] the ligand mixed (mono Schiff base-

ONX)(trithiocyanato-*N*)chromium(III) complexes were produced. All the complexes have *mer*-octahedral structures which were in the case of three complexes proved by X-ray analyses. By solving the crystal structures of two different forms of PLSC ligand, neutral PLSC·2H₂O and protonated PLSC·HNCS, it was found that PLSC·HNCS has the same (*cis*) position of donor atoms as in the complexes, which is not the case with its neutral form.

Acknowledgments

The research was supported by the Ministry of Education and Science, of the Republic of Serbia (Grant no. 172014) and the Provincial Secretariat for Science and Technological Development of Vojvodina.

References

- [1] S. Praveen Kumar, R. Suresh, K. Giribabu, R. Manigandan, S. Munusamy, S. Muthamizh, V. Narayanan, Spectrochim. Acta A139 (2015) 431.
- [2] M. Cindrić, M. Rubčić, Croat. Chem. Acta 85 (2012) 505.
- [3] V.G. Vaidyanathan, T. Weyhermuller, B. Unni Nair, J. Subramanian, J. Inorg. Biochem. 99 (2005) 2248.
- [4] K.A. Biedermann, J.R. Landolph, Cancer Res. 50 (1990) 7835.
- [5] M.J.M. Campbell, Coord. Chem. Rev. 15 (1975) 279.
- [6] S. Padhye, G.B. Kauffman, Coord. Chem. Rev. 63 (1985) 127.
- [7] J.S. Casas, M.S. Garcia-Tacende, J. Sordo, Coord. Chem. Rev. 209 (2000) 197.
- [8] T.S. Lobana, R. Sharma, G. Bawa, S. Khanna, Coord. Chem. Rev. 253 (2009) 977.
- [9] D.X. West, S.B. Padhye, P.B. Sonawane, Struct. Bond 76 (1991) 1.
- [10] H. Beraldo, D. Gambino, Mini-Rev. Med. Chem. 4 (2004) 31.
- [11] R.B. Singh, B.S. Garg, R.P. Singh, Talanta 25 (1978) 619.
- [12] R.B. Singh, H. Ishii, Cryt. Rev. Anal. Chem. 22 (1991) 381.
- [13] V.M. Leovac, V.S. Jevtović, Lj.S. Jovanović, G.A. Bogdanović, J. Serb. Chem. Soc. 70 (2005) 393.
- [14] M. Belicchi-Ferrari, F. Bisceglei, C. Casoli, S. Durot, I. Morgestern-Badarau, G. Pelosi, E. Pilotti, S. Pinelli, P. Tarasconi, J. Med. Chem 48 (2005) 1671.
- [15] M.R. Maurya, A. Kumar, M. Abid, A. Azam, Inorg. Chim. Acta. 359 (2006) 2439.
- [16] J.S Casas, M.D. Couce, J. Sordo, Coord. Chem. Rev 256 (2012) 3036.
- [17] D. Vidović, A. Radulović, V. Jevtović, Polyhedron 30 (2011) 16.
- [18] E.W. Yemeli Tido, C. Faulmann, R. Roswanda, A. Meetsma, P.J. van Koningsbruggen, Dalton Trans. (2010) 1643.
- [19] M. Mohan, P.H. Madhuranath, A. Kumar, M. Kumar, N.K. Jha, Inorg. Chem. 28 (1989) 96.
- [20] N.Ž. Knežević, V.M. Leovac, V.S. Jevtović, S. Grgurić-Šipka, T.J. Sabo, Inorg. Chem. Comm. 6 (2003) 561.
- [21] CrysAlisPro Software system, Agilent Technologies UK Ltd., Oxford, 2014.

- [22] G.M. Sheldrick, *Acta Crystallogr., Sect. A* 71 (2015) 3–8.
- [23] G.M. Sheldrick, *Acta Crystallogr., Sect. C* 71 (2015) 3–8.
- [24] C.B. Hübschle, G.M. Sheldrick, B. Dittrich, *J. Appl. Crystallogr.* 44 (2011) 1281.
- [25] A.L. Spek, *Acta Crystallogr., Sect. D* 65 (2009) 148.
- [26] F.H. Allen, *Acta Crystallogr., Sect. B* 58 (2002) 380.
- [27] C.F. Macrae, I.J. Bruno, J.A. Chisholm, P.R. Edgington, P. McCabe, E. Pidcock, L. Rodriguez-Monge, R. Taylor, J. van de Streek, P.A. Wood, *J. Appl. Crystallogr.* 41 (2008) 466.
- [28] W.J. Geary, *Coord. Chem. Rev.* 7 (1971) 81.
- [29] V.M. Leovac, M.D. Joksović, V. Divjaković, Lj.S. Jovanović, Ž. Šaranović, A. Pevec, *J. Inorg. Biochem.* 101 (2007) 1094.
- [30] P. Kalaivani, R. Prabhakaran, E. Ramachandran, F. Dallemer, G. Paramaguru, R. Renganathan, P. Poornima, V. Vijaya Padma, K. Natarajan, *Dalton Trans.* 41 (2012) 2486.
- [31] S. Ivković, Lj.S. Vojinović-Ješić, V.M. Leovac, M.V. Rodić, S.B. Novaković, G.A. Bogdanović, *Struct. Chem.* 26 (2015) 269.
- [32] M. Belicchi-Ferrari, G.F. Gasparri, E. Leporati, C. Pelizzi, P. Tarasconi, G. Tosi, *J. Chem. Soc. Dalton Trans.* (1986) 2455.
- [33] P.-D. Pilar, P. Souza, J.R. Masaguer, A. Arquero, *Transition Met. Chem.* 12 (1987) 200.
- [34] T. Ghosh, S. Bhattacharya, A. Das, G. Mukherjee, M.G.B. Drew, *Inorg. Chim. Acta* 358 (2005) 989.
- [35] M.R. Maurya, S. Khurana, W. Zhang, D. Rehder, *J. Chem. Soc., Dalton Trans.* (2002) 3015.
- [36] A. Syamal, M.R. Maurya, *Transition Met. Chem.* 11 (1986) 235.
- [37] S. Floquet, M. Carmen Munoz, R. Guillot, E. Riviere, G. Blain, J.A. Real, M.L. Boillot, *Inorg. Chim. Acta* 362 (2009) 56.
- [38] K. Nakamoto, *Infrared and Raman Spectra of Inorganic and Coordination Compounds Part B*, Wiley, Hoboken, New Jersey, 2009.
- [39] V.S. Jevtović, Lj.S. Jovanović, V.M. Leovac, L.J. Bjelica, *J. Serb. Chem. Soc.* 68 (2003) 929.
- [40] T.-F. Liu, H.-Y. Lv, B.-T. Zhao, J.-G. Wang, *Acta Crystallogr., Sect. E* 63 (2007) m2406.
- [41] S.K. Padhi, D. Saha, R. Sahu, J. Subramanian, V. Manivannan, *Polyhedron* 27 (2008) 1714.
- [42] Yu.M. Chumakov, V.I. Tsapkov, P.A. Petrenko, S.A. Palomares-Sánchez, A.P. Gulea, *J. Struct. Chem* 54 (2013) 824.
- [43] B. Shaabani, A.A. Khandar, M. Dusek, M. Pojarova, F. Mahmoudi, *Inorg. Chim. Acta* 394 (2013) 563.
- [44] P. Sonawane, R. Chikate, A. Kumbhar, S. Padhye, *Polyhedron* 13 (1994) 395.
- [45] U.L. Kala, S. Suma, M.R.P. Kurup, S. Krishnan, R.P. John, *Polyhedron* 26 (2006) 1427.
- [46] B. Shaabani, A. A. Khandar, F. Mahmoudi, M. A. Maestro, S. S. Balula, L. Cunha-Silva, *Polyhedron* 57 (2013) 118.

- [47] G.A. Bogdanović, V.M. Leovac, Lj.S. Vojinović-Ješić, A.S. Biré, J. Serb. Chem. Soc. 72 (2007) 63.
- [48] A.M.B. Bastos, J.G. da Silva, P.I. da S. Maia, V.M. Deflon, A. Batista, A.V.M. Ferreira, L.M. Botion, E. Niquet, H. Beraldo, Polyhedron 27 (2008) 1787.
- [49] R.P. John, A. Sreekanth, M.R.P. Kurup, H.-K. Fun, Polyhedron 24 (2005) 601.
- [50] H. Bashir Shawish, M. Paydar, C.Y. Looi, Y.L. Wong, E. Movahed, S.N.A. Halim, W.F. Wong, M.-R. Mustafa, M.J. Maah, Transition Met. Chem. 39 (2014) 81.
- [51] M.M. Lalović, Lj.S. Jovanović, Lj.S. Vojinović-Ješić, V.M. Leovac, V.I. Češljević, M.V. Rodić, V. Divjaković, J. Coord. Chem. 65 (2012) 4217.
- [52] Lj. Jovanović, Ph.D. thesis, Faculty of Sciences, Novi Sad, 1986.
- [53] T.V. Troepol'skaya, G.K. Budnikov, Elektrokimiya azometinov, Nauka, Moskva, 1989.
- [54] G.K. Budnikov, Elektrokhimicheskie reaktsii khelatov metallov v organicheskikh i smeshannykh rastvoritelyakh, Izd. Kazanskogo univ., 1980.
- [55] I.B. Rietveld, R. Céolin, J. Therm. Anal. Calorim., 120 (2015) 1079.
- [56] P.S. Binil, M.R. Anoop, S. Suma, M.R. Sudarsanakumar, J. Therm. Anal. Calorim., 112 (2013) 913.
- [57] S. Packiaraj, A. Pushpaveni, C. Senthil, S. Govindarajan, J. M. Rawson, J Therm. Anal. Calorim., 119 (2015) 15.
- [58] A. Czyłkowska, J. Therm. Anal. Calorim. DOI 10.1007/s10973-015-4673-2.
- [59] <http://webbook.nist.gov/> access: 15.05.2015.

Table 1. Crystallographic data for PLSC·2H₂O, PLSC·HNCS and complexes **2**, **4**, **5**

	PLSC·2H ₂ O	PLSC·HNCS	2	4	5
CCDC No.					
Molecular formula	C ₉ H ₁₆ N ₄ O ₅	C ₁₀ H ₁₃ N ₅ O ₃ S	C ₁₄ H ₁₇ N ₇ O ₄ S ₃ KCr	C ₁₈ H ₂₄ N ₁₁ O ₁₃ S ₂ Cr	C ₁₂ H ₁₆ N ₇ O ₄ S ₄ Cr
<i>M</i> (g mol ⁻¹)	260.26	283.31	534.63	718.6	502.56
Crystal system	Monoclinic	Triclinic	Monoclinic	Triclinic	Orthorhombic
Space group	<i>P</i> 2 ₁ / <i>c</i>	<i>P</i> $\bar{1}$	<i>P</i> 2 ₁ / <i>n</i>	<i>P</i> $\bar{1}$	<i>Pna</i> 2 ₁
<i>a</i> (Å)	11.6462(9)	4.9927(4)	8.5575(2)	7.9946(3)	17.2793(4)
<i>b</i> (Å)	7.1123(5)	8.5183(6)	15.8793(4)	11.1599(5)	14.2138(4)
<i>c</i> (Å)	14.5095(10)	15.7383(11)	16.0153(4)	17.2273(7)	8.5423(2)
α (°)	90	74.639(6)	90	71.899(4)	90
β (°)	101.217(7)	89.759(6)	96.520(2)	89.255(3)	90
γ (°)	90	83.499(8)	90	73.877(4)	90
<i>V</i> (Å ³)	1178.88(15)	641.05(8)	2162.20(9)	1398.94(11)	2098.02(9)
<i>Z</i>	4	2	4	2	4
<i>D</i> _{calc} (g cm ⁻³)	1.466	1.468	1.624	1.706	1.591
μ (mm ⁻¹)	1.029 (Cu <i>K</i> α)	2.39 (Cu <i>K</i> α)	9.12 (Cu <i>K</i> α)	0.64 (Mo <i>K</i> α)	8.52 (Cu <i>K</i> α)
<i>F</i> (000)	552	296	1068	738	1028
Crystal size (mm)	0.69 × 0.09 × 0.09	0.35 × 0.15 × 0.08	0.41 × 0.13 × 0.07	0.4 × 0.24 × 0.03	0.54 × 0.19 × 0.03
Color / Shape	Yellow / Prism	Yellow / Irregular	Dark red / Prism	Dark red / Plate	Dark red / Plate
Temperature (K)	298(2)	294(2)	298(2)	294(2)	298(2)
Radiation type; λ (Å)	Cu <i>K</i> α ; 1.5418	Cu <i>K</i> α ; 1.5418	Cu <i>K</i> α ; 1.5418	Mo <i>K</i> α ; 0.71073	Cu <i>K</i> α ; 1.5418
θ range (°)	3.9–67.0	2.9–67.0	3.9–72.5	3.0–30.7	4.0–72.4
No. reflections; unique	4025; 2100	3677; 2271	8101; 4173	25865; 7824	13744; 2986
<i>R</i> _{int}	0.024	0.021	0.022	0.026	0.030
No. observed reflections	1654	1960	3651	6456	2831
Restraints; parameters	11; 192	24; 204	41; 294	0; 447	12; 282
Goodness-of-fit on <i>F</i> ²	1.05	1.05	1.08	1.126	1.05
<i>R</i> ; <i>wR</i> [<i>F</i> _o > 4 σ (<i>F</i> _o)]	0.041 / 0.10	0.041 / 0.109	0.044 / 0.113	0.038 / 0.11	0.028 / 0.075
<i>R</i> ; <i>wR</i> [all data]	0.054 / 0.11	0.047 / 0.11	0.051 / 0.118	0.053 / 0.13	0.031 / 0.077
$\Delta\rho_{\max}$ and $\Delta\rho_{\min}$ (e Å ⁻³)	0.23 and -0.19	0.26 and -0.24	0.62 and -0.62	0.68 and -0.57	0.31 and -0.25

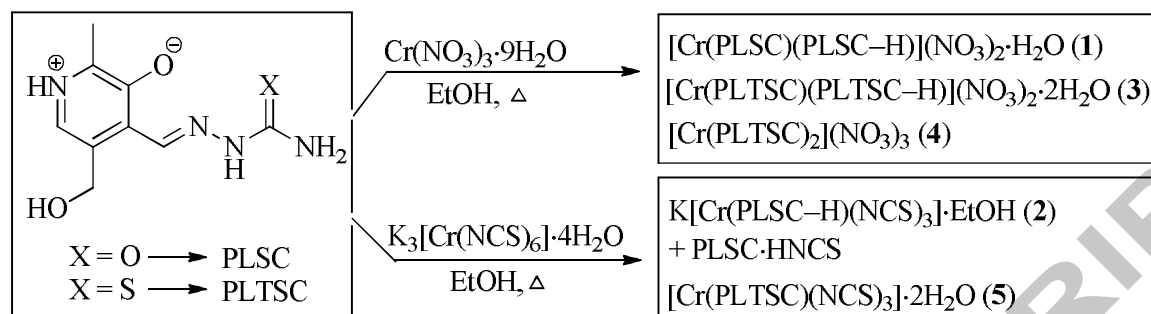
Table 2. Selected structural data (Å, °) for PLSC·2H₂O, PLSC·HNCS, and complexes **2**, **4**, and **5**

Bonds	PLSC·2H ₂ O	PLSC·HNCS	2	4	5
Cr1–O2	–	–	1.913(2)	1.9131(15)	1.933(2)
Cr1–O2A	–	–	–	1.9356(14)	–
Cr1–N3	–	–	1.992(2)	2.0322(16)	2.041(3)
Cr1–N3A	–	–	–	2.0345(15)	–
Cr1–X1*	–	–	1.9800(19)	2.3905(6)	2.3821(11)
Cr1–S1A	–	–	–	2.3905(6)	–
Cr1–N5	–	–	2.007(2)	–	1.986(3)
Cr1–N6	–	–	2.009(3)	–	2.000(3)
Cr1–N7	–	–	2.019(3)	–	2.000(3)
C1–N1	1.328(5)	1.334(9)	1.338(4)	1.310(3)	1.316(5)
C1A–N1A	–	–	–	1.312(3)	–
C1–X1*	1.247(4)	1.217(8)	1.300(4)	1.711(2)	1.700(4)
C1A–S1A	–	–	–	1.708(2)	–
C1–N2	1.371(5)	1.390(8)	1.330(4)	1.346(3)	1.339(5)
C1A–N2A	–	–	–	1.346(3)	–
N2–N3	1.362(4)	1.340(7)	1.385(4)	1.380(2)	1.370(4)
N2A–N3A	–	–	–	1.371(2)	–
C2–N3	1.266(5)	1.277(8)	1.289(4)	1.296(3)	1.291(4)
C2A–N3A	–	–	–	1.288(2)	–
C4–O2	1.295(4)	1.337(7)	1.302(4)	1.304(2)	1.301(4)
C4A–O2A	–	–	–	1.300(2)	–
O2–Cr1–X1*	–	–	169.88(8)	170.70(4)	172.53(8)
O2A–Cr1–S1A	–	–	–	169.91(5)	–
N3–Cr1–N3A	–	–	–	175.69(7)	–
N6–Cr1–N7	–	–	179.28(11)	–	177.08(14)
N3–Cr1–N5	–	–	172.64(10)	–	173.33(13)
C5–N4–C7	124.2(3)	124.3(6)	123.8(3)	124.42(19)	125.3(3)
C5A–N4A–C7A	–	–	–	124.66(18)	–
τ (C3–C4–O2–Cr1)	–	–	6.5(4)	–32.3(3) –39.2(3)	18.1(5)
τ (C1–N2–N3–Cr1)	–	–	–3.0(3)	26.3(2) 23.3(2)	–11.3(4)
δ^{**}	–	–	8.7(2)	31.62(6) 24.23(4)	14.32(13)

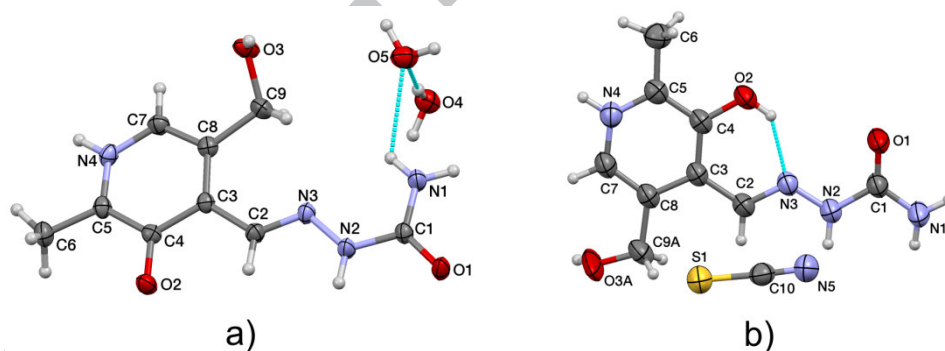
* X = O in PLSC·2H₂O, PLSC·HNCS, and **2**; X = S in **4** and **5**.

**dihedral angle between mean plane of pyridine ring and mean plane through donor atoms of chelate ligand and Cr1

Figures



Scheme 1. Preparation routes to the Cr(III) complexes

Figure 1. Molecular structures of PLSC·2H₂O (a), and PLSC·HNCS (b)

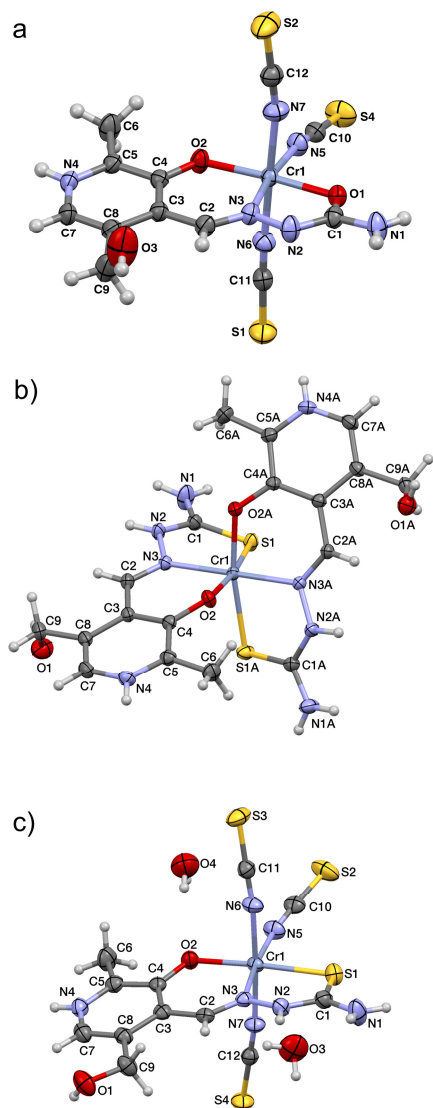


Figure 2. Structures of: (a) anionic part of **2** $[\text{Cr}(\text{PLSC-H})(\text{NCS})_3]^-$; (b) cationic part of **4** $[\text{Cr}(\text{PLTSC})_2]^{3+}$; (c) $[\text{Cr}(\text{PLTSC})(\text{NCS})_3] \cdot 2\text{H}_2\text{O}$ (**5**)

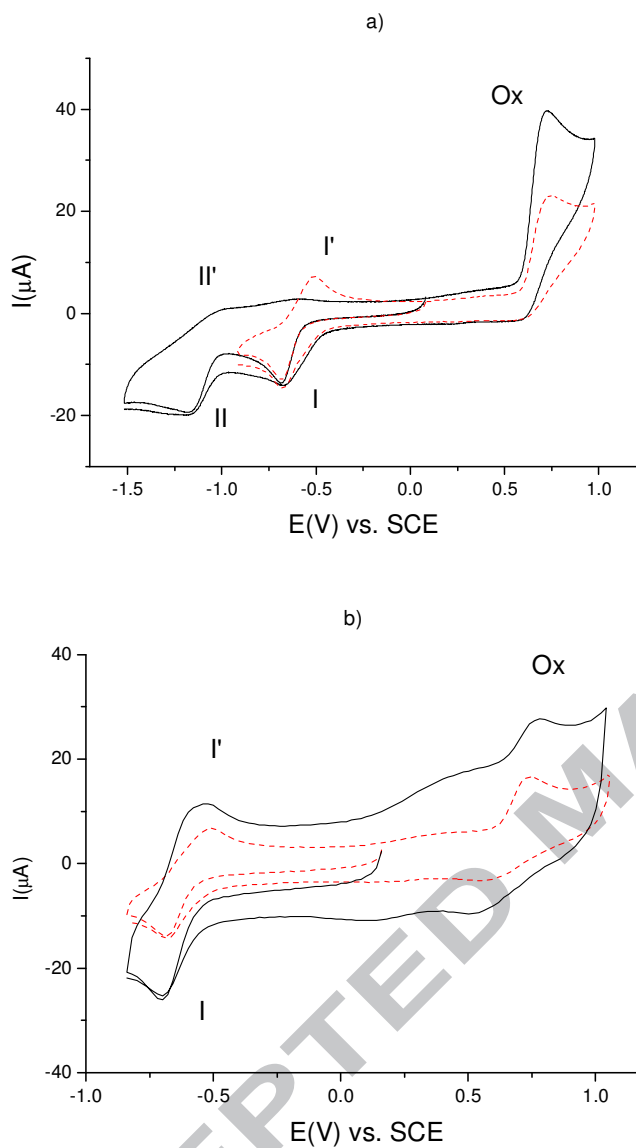


Figure 3. a) Cyclic voltammograms for $\text{K}[\text{Cr}(\text{PLSC-H})(\text{NCS})_3] \cdot \text{EtOH}$; DMF+0.1 M TBAP, GC, 0.10 V s^{-1} . $c = 1.12 \text{ mM}$. b) Cyclic voltammograms for $\text{K}[\text{Cr}(\text{PLSC-H})(\text{NCS})_3] \cdot \text{EtOH}$; DMF+0.1 M TBAP, GC, 0.50 V s^{-1} (dashed line) and 2 V s^{-1} (solid line) $c = 0.58 \text{ mM}$

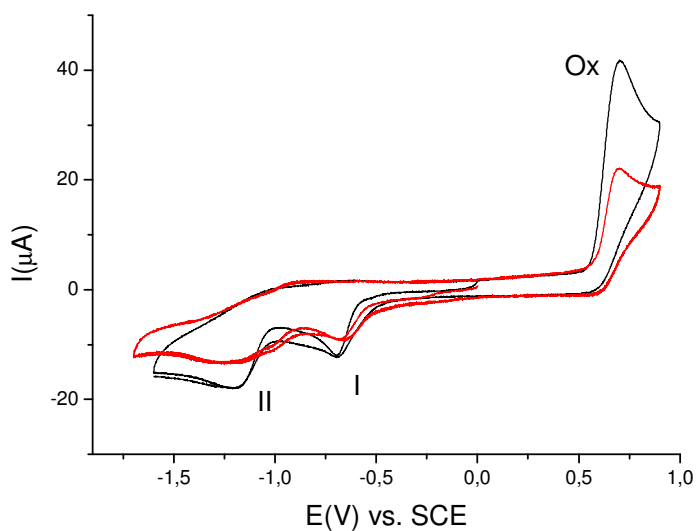


Figure 4. Cyclic voltammograms for $\text{K}[\text{Cr}(\text{PLSC-H})(\text{NCS})_3] \cdot \text{EtOH}$ (solid line, $c = 1.12 \text{ mM}$) and for $[\text{Cr}(\text{PLTSC})(\text{NCS})_3] \cdot 2\text{H}_2\text{O}$ (dashed line, $c = 0.86 \text{ mM}$); DMF+0.1 M TBAP, GC, 0.10 V s^{-1} .

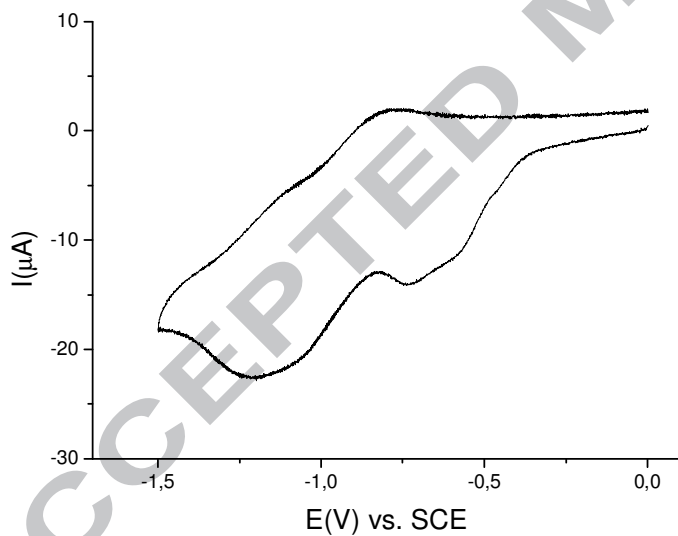


Figure 5. Cyclic voltammograms for $[\text{Cr}(\text{PLTSC})(\text{PLTSC-H})(\text{NO}_3)_2] \cdot 2\text{H}_2\text{O}$ ($c = 1.49 \text{ mM}$); DMF+0.1M TBAP, GC, 0.10 V s^{-1} .

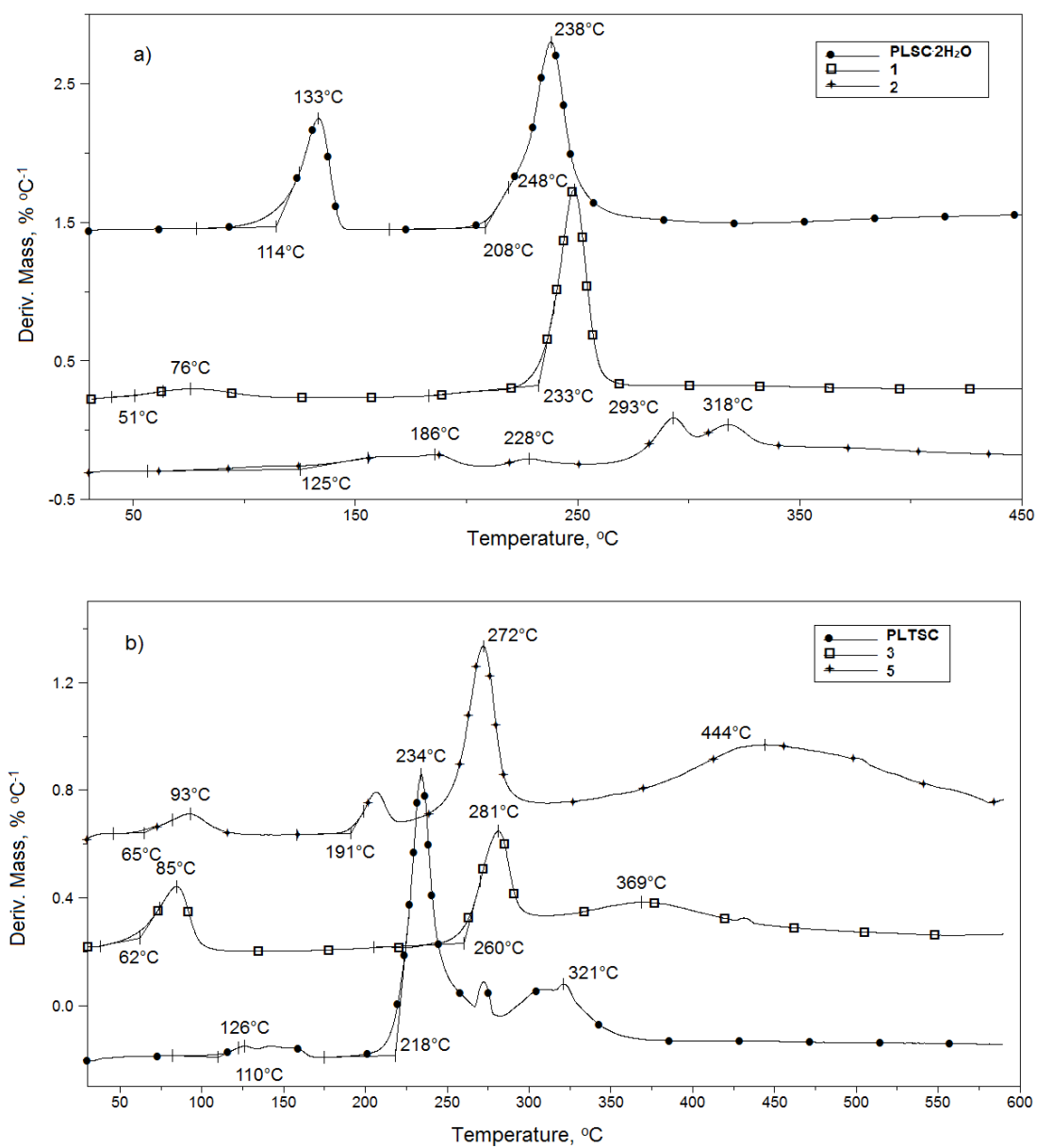


Figure 6. a) DTG curves of PLSC, **1** and **2**. b) DTG curves of PLTSC, **3** and **5**.

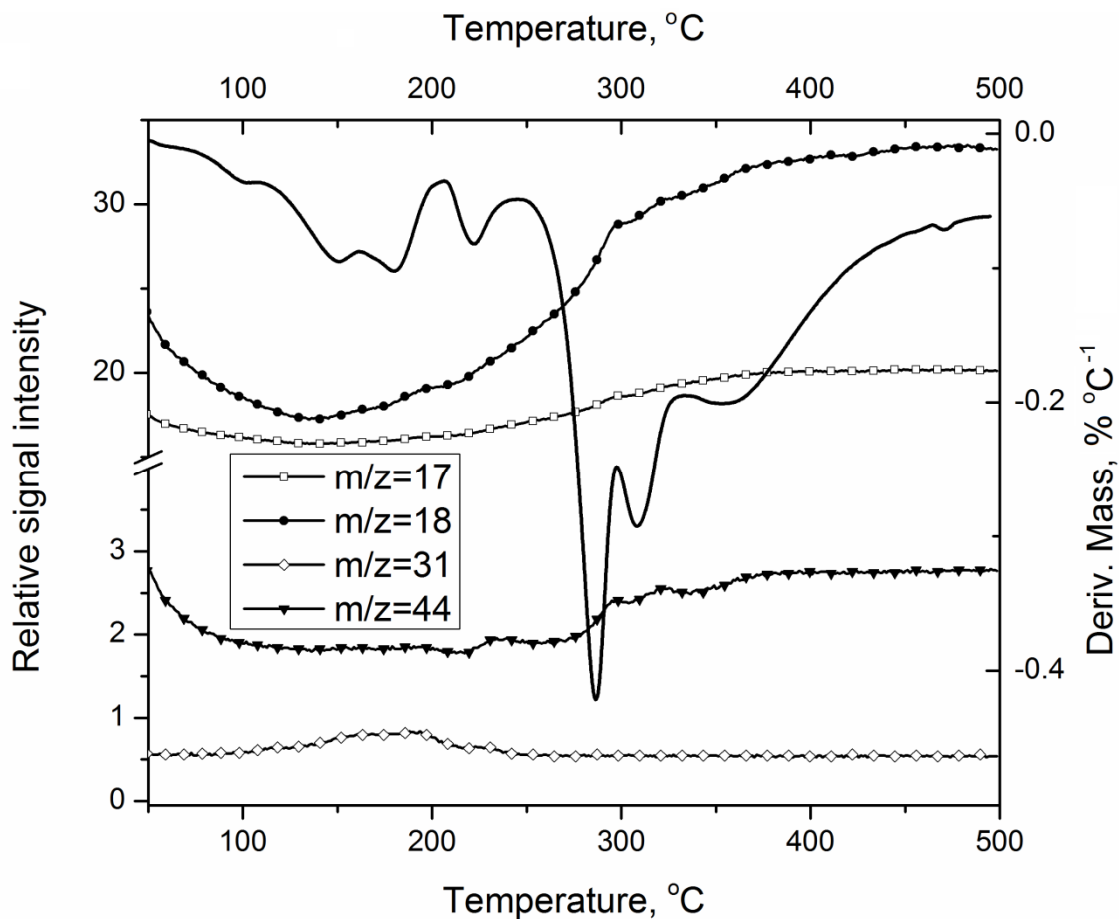


Figure 7. DTG/MS data for EtOH evaporation ($m/z = 31$) and selected fragments for the decomposition of **2** in flowing argon. Graphical abstract

Five Cr(III) complexes with tridentate ONX (X = O, S) ligands, i.e. pyridoxal semi-/thiosemicarbazones, being the first complexes with these ligands, were synthesized and characterized. All the complexes have *mer*-octahedral structures, which in the case of **2**, **4**, **5**, were proved by single crystal X-ray analysis. Detailed electrochemical and thermal analyses of the studied compounds were performed.

Synopsis

ACCEPTED MANUSCRIPT